

Hole-Free Phase Plate Imaging of a Phase Grating

Marek Malac^{1,2}, Misa Hayashida¹, Ken Harada³, Keiko Shimada³, Kodai Niitsu³, Teddy Rowan¹ and Marco Beleggia⁴

¹. Nanotech. Res. Centre, Nat. Research Council, Edmonton, Canada.

². Department of Physics, University of Alberta, Edmonton, Canada.

³. RIKEN, Hatoyama, Saitama, Japan.

⁴. Center for Electron Nanoscopy, Technical University of Denmark, Lyngby, Denmark.

Hole free phase plate (HFPP) imaging provides a convenient way to enhance phase contrast in a TEM [1]. HFPP imaging applications range from biology to magnetic materials, but quantitative image interpretation has not been possible so far [1,2,3]. Here we present a detailed study of HFPP images of a FIB-fabricated phase grating that allows us to study how the HFPP modifies the phase relationship between direct and diffracted beams.

Diffraction grating grooves were milled by Ga⁺ beam in a Hitachi NB-5000 FIB/SEM into ~13 nm thick amorphous Si. The grating periodicity was 98 nm, see Fig. 1a. The sample was observed at 300 kV in a cold-FEG Hitachi HF-3300S TEM with two sample positions. The grating was placed in the upper sample position while a 13 nm carbon film, the HFPP, was placed in a heating holder at T=150 C in the lower sample position. The microscope optics was adjusted to form the diffraction pattern of the grating at the HFPP plane, with a separation between the first two diffracted beams of ~1.5 μm (equivalent to a camera length of 37 cm). This way the contribution of the direct and diffracted beams to the image contrast can be separated, Fig. 1b. Electron holography (EH) was used to measure the phase shift induced the direct and diffracted beam locations at the HFPP after the grating was removed, Fig 1b.

Fig 2a shows intensity profile evolution extracted a time series of images of the grating. Contrast reversals with time (i.e. with dose) at HFPP can be clearly observed in 2b. The phase profile at the HFPP in Fig 1b appears broader than the beam current profile, with a net phase shift of the diffracted beams comparable to that of the direct beam even if the current carried by the direct beam is 213x higher than each of the 1st order diffracted beams. The 2nd order diffracted beams are 6965x lower than the direct beam and were neglected in simulations. The magnitude of the direct beam phase shift (~0.6 rad) being only about 2-3 times larger than the side beams phase shift (~0.2-0.3 rad) while the beam current is 213x higher at the direct beam suggests a saturation mechanism affecting the phase shift [5]. EH confirms that the phase shift was negative [3,4,5,6].

Fig 3 shows a simulation of the image intensity evolution that can be compared to the experimental data in Fig 2. The Lorentzian-shaped phase shift of each beam at the HFPP was assumed to evolve exponentially with time t , according to $\Phi_{DB}[1 - \text{Exp}(-t/\tau_{DB})]$ and $\Phi_{SB}[1 - \text{Exp}(-t/\tau_{SB})]$ for direct and side (diffracted) beams, respectively. The sign convention from [6] was used. The time constants were taken: $\tau_{DB}/\tau_{SB}=200 \text{ s} / 300 \text{ s}$ and the ratio of the magnitude was taken as $\Phi_{SB}/\Phi_{DB} = 1 / 3$, as measured by EH. Fig 3a) shows the time evolution of phase shift at HFPP. Fig 3b) shows image intensity and c) intensity profile evolution. Comparison to Fig 2a and 2b indicates that the contrast reversals are captured in the simulation although the simulation. Contrast reversal occurs when $\Delta\Phi = \Phi_{DB} - \Phi_{SB} = n\pi$, with integer n ; when n is odd, contrast reversal is accompanied by frequency doubling of the observed fringe pattern, in agreement with experiment.

Using a diffraction grating sample, it was possible to separate the effect of charging at the direct and diffracted beam locations of HFPP. The salient features of the image contrast evolution with dose were reproduced by a scenario when the HFPP under the direct beam charges faster and achieves a larger net phase shift than under the diffracted beams.

References:

[1] Malac *et al.*, Ultramicroscopy **118** (2012), p. 77.
 [2] Malac *et al.*, Appl. Phys. Lett. **102** (2013), p. 192401.
 [3] Danev *et al.*, PNAS **111** (2014), p. 15635.
 [4] Hettler *et al.*, Micron **96** (2017), p. 38.
 [5] Hettler *et al.*, Ultramicroscopy **184** (2018), p. 252.
 [6] Malac *et al.*, Micron **100** (2017), p. 10.

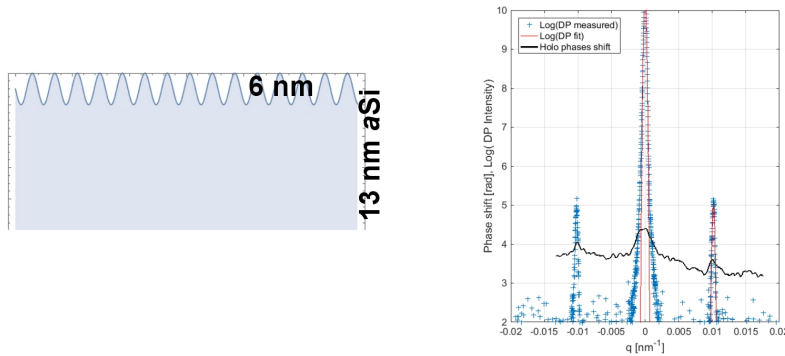


Figure 1 a) Schematic indication of the sample. A 13 nm amorphous Si with ~1 nm deep grooves fabricated by a focused ion beam instrument b) measured beam intensity at HFPP (+, blue), fitted intensity at HFPP (red solid) and electron holography phase shift measurement at HFPP (solid black).

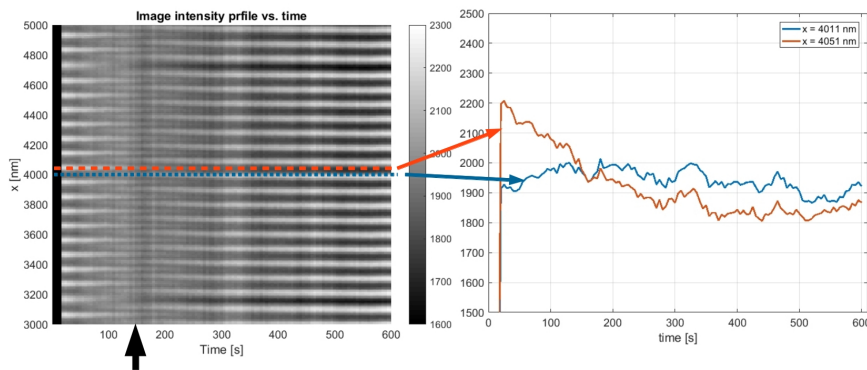


Figure 2 a) Evolution of intensity profile extracted from experimental dose series of grating images. b) intensity evolution from a location of the profile a) that corresponds to maximum and minimum initial intensity. The contrast reversal is marked by an arrow.

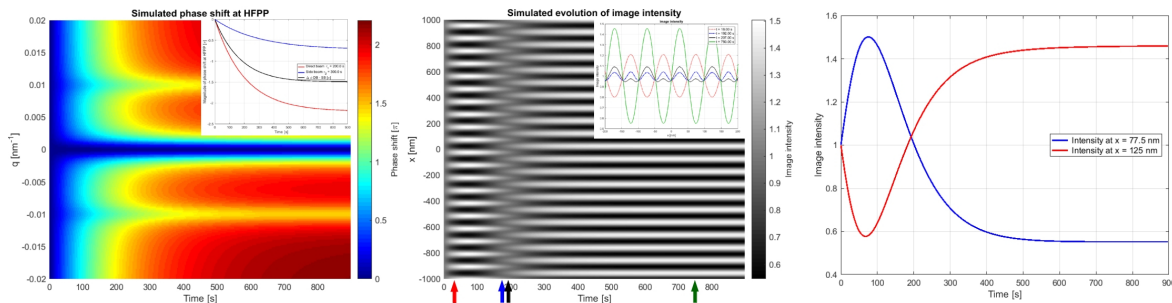


Figure 3 Simulated a) phase shift evolution at the HFPP, the inset indicates the magnitude of phase shift of direct beam (lower, red curve), diffracted beam (upper, blue curve) and their difference (black, middle) with time. b) Simulated image intensity evolution and intensity profile c), as function of time. The inset in b) shows intensity profiles at time marked by arrows.